

# Entanglement and lasing with two quantum dots in a microcavity

Elena del Valle,<sup>1</sup> F. P. Laussy,<sup>1</sup> F. Troiani,<sup>2</sup> and C. Tejedor<sup>1</sup>

<sup>1</sup>Departamento de Física Teórica de la Materia Condensada, Universidad Autónoma de Madrid, Cantoblanco 28049 Madrid, Spain

<sup>2</sup>CNR-INFM National Research Center on nanoStructures and bioSystems at Surfaces (S3), 41100 Modena, Italy

(Received 14 June 2007; published 19 December 2007)

Entanglement and lasing of two quantum dots in a microcavity are investigated in the steady state achieved under a continuous incoherent pumping. Lasing is favored in the case of independent pumping of the dots, i.e., when an electron-hole pair which reaches one dot does not affect the other. In this case, having two dots allows a qualitative enhancement of the lasing emission as compared to the single dot case. On the other hand, when the two dots share the excitation bath, giving rise to a quantum uncertainty of the final state of the excitation, entanglement properties are enhanced in detriment of the photon emission. Slightly different couplings between the dots and the cavity induce good singlet-state population. This allows good entanglement in a system pumped continuously and incoherently.

DOI: [10.1103/PhysRevB.76.235317](https://doi.org/10.1103/PhysRevB.76.235317)

PACS number(s): 78.67.Hc, 42.50.Dv, 03.67.Hk

## I. INTRODUCTION

Semiconductor nanostructures offer great possibilities as physical support for light-matter interaction:<sup>1,2</sup> quantum wells, quantum dots (QDs), and optical cavities can be monolithically fabricated, making them suitable for integration in scalable devices. The use of QDs, rather than atoms, as photoemitters allows electrical injection as well as repeating an experiment with the same sample. This removes the need for complicated trapping techniques, and opens the possibility of tuning the energies of the different excitations.<sup>3</sup> For instance, an optimum and deterministic coupling between a single cavity mode and QD excitons has been achieved recently by placing the QD at the antinode of the electromagnetic field.<sup>4,5</sup>

Unlike atoms, QDs are not identical to each other. Self-assembled QDs are randomly distributed in space and present a small size inhomogeneity. This results in a finite dispersion in the coupling to the cavity modes and in the emission frequency. The aim of the present work is to analyze the effect of such differences. In particular, we show how one can take advantage of them to engineer the emission of the structure, its lasing properties, or the generation of entangled states. For this purpose, we study the case of two QDs, each one represented as a two-level system,<sup>6,7</sup> close to resonance with the single mode of a microcavity. In this simple model, we are neglecting internal degrees of freedom such as carrier spin or photon polarization, which can be achieved, for instance, by working with charged QDs. Our main finding is that, depending on how the two QDs are pumped, in a sense that we explain below, one can obtain configurations with either a high degree of entanglement or good lasing properties.

The paper is organized as follows. In Sec. II, the model Hamiltonian is introduced and a master equation is derived for two pumping configurations. In Sec. III, the potentiality of the system for entangling two equal QDs is discussed and analyzed through its tangle and entropy. In Sec. IV, the lasing properties are analyzed through the photon population and the second-order coherence. Section V provides the conclusions.

## II. DESCRIPTION OF THE SYSTEM

We describe the QDs as two-level systems, with excitation frequencies  $\omega_{i=1,2}$  and detunings with respect to the cavity mode  $\Delta_i = \omega - \omega_i$  ( $\hbar = 1$ ). The QD Hilbert space is spanned by a “localized” basis  $\{|0\rangle = |G_1, G_2\rangle, |1\rangle = |E_1, G_2\rangle, |2\rangle = |G_1, E_2\rangle, |3\rangle = |E_1, E_2\rangle\}$ , where  $|G_i\rangle$  and  $|E_i\rangle$  are the vacuum and exciton states, respectively, of dot  $i$ . Alternatively, one can refer to the Dicke states, corresponding to the three triplet states  $\{|T_{-1}\rangle = |0\rangle, |T_0\rangle = \frac{1}{\sqrt{2}}(|1\rangle + |2\rangle), |T_1\rangle = |3\rangle\}$  and to the singlet state  $\{|S\rangle = \frac{1}{\sqrt{2}}(|1\rangle - |2\rangle)\}$ .

The dot-cavity coupling takes the Jaynes-Cummings form,<sup>8</sup> with parameters  $g_i$ . The system Hamiltonian therefore reads

$$\hat{H}_0 = \omega \hat{a}^\dagger \hat{a} + \sum_{i=1,2} \left[ \frac{(\omega - \Delta_i)}{2} \hat{\sigma}_i^z + g_i (\hat{a} \hat{\sigma}_i^+ + \hat{a}^\dagger \hat{\sigma}_i^-) \right]. \quad (1)$$

Here,  $\hat{a}$  is the cavity-photon annihilation operator,  $\hat{\sigma}_i^{x,y,z}$  are the Pauli matrices in the  $\{|G_i\rangle, |E_i\rangle\}$  basis, and  $\hat{\sigma}_i^\pm = \hat{\sigma}_i^x \pm i \hat{\sigma}_i^y$ .

In the Dicke basis, the interaction part of  $\hat{H}_0$  becomes

$$\hat{H}_{\text{int}} = g \hat{a} (|T_0\rangle \langle T_{-1}| + |T_1\rangle \langle T_0|) + \text{H.c.} + \delta g \hat{a} (|S\rangle \langle T_{-1}| - |T_1\rangle \langle S|) + \text{H.c.}, \quad (2)$$

where  $g = (g_1 + g_2) / \sqrt{2}$  and  $\delta g = (g_1 - g_2) / \sqrt{2}$ . Figure 1 shows the corresponding level scheme, up to two excitations in the Dicke basis, with all the coherent and incoherent couplings, represented by curved and straight arrows, respectively. Note that when  $g_1 = g_2$ , the singlet state decouples from the other ones and becomes a *dark state*. This will play an important role in what follows. The interaction with the environment (that is, the leakage of the cavity photons and the incoherent pumping of the QDs) causes the system to evolve into a mixed state. Its dynamics must, thus, be analyzed in terms of the density matrix operator  $\hat{\rho}$  of the two-QD plus cavity degrees of freedom. Its temporal evolution is given by the master equation that is obtained within the Born-Markov and secular approximations.<sup>7,9,10</sup> Incoherent contributions are expressed in the form of Lindblad terms, which are Liouvillean superoperators applied on the density matrix. The equation

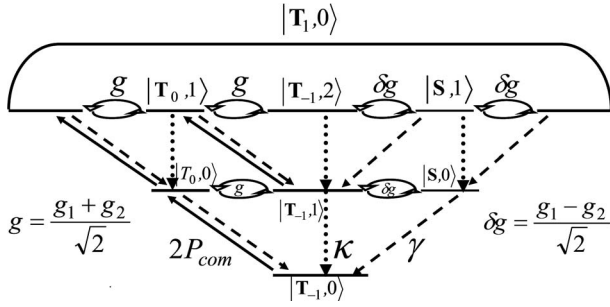


FIG. 1. Levels of the system up to two excitations in Dicke basis. Only the case with common pumping bath ( $P_{\text{ind}}=0$ ) is presented here in order to illustrate the discussion in Sec III. Solid lines represent the common pump, which only affects the triplet subspace  $|T_{-1}, n\rangle$ ,  $|T_0, n\rangle$ , and  $|T_1, n\rangle$  with  $2P_{\text{com}}$ , increasing the dot excitations without changing the number of photons  $n$ . Dotted lines stand for the cavity photon decay. Dashed lines take account of the leaky modes affecting all QD levels. Finally, curved arrows show coherent couplings ( $g$  and  $\delta g$ ) between levels.

of motion reads  $d\hat{\rho}/dt = i[\hat{\rho}, \hat{H}_0] + \frac{\chi}{2}\mathcal{L}\hat{\rho}$ , where the superoperator  $\mathcal{L}\hat{\rho} = 2\hat{O}\hat{\rho}\hat{O}^\dagger - \hat{O}^\dagger\hat{O}\hat{\rho} - \hat{\rho}\hat{O}^\dagger\hat{O}$  corresponds to the general deexcitation operator  $\hat{O}$  and its effective decaying rate  $\chi$ . The escape of the cavity photons is accounted for by a Lindblad term  $\mathcal{L}_\kappa\hat{\rho}$ , with a rate  $\chi = \kappa$ . This parameter is inversely proportional to the cavity quality factor  $Q$ :  $\kappa = \omega/Q$ .<sup>2</sup> The spontaneous decay of the QD excited state into any other mode than the one of the cavity as well as the nonradiative decay are taken into account with the term  $\mathcal{L}_\gamma\hat{\rho}$  and associated rates  $\gamma$ . Such rates are typically much below the cavity emission rate  $\kappa$ . Still they can induce significant deviations from the ideal case and should be included. In this paper, the leaky parameter is set to  $\gamma = 5 \times 10^{-3}$ . We neglect pure dephasing of the QDs for simplicity.

The last essential ingredient is the excitation of the QDs. Here, these are pumped continuously and incoherently. Experiments usually excite far above resonance by electron-hole pair injection to the wetting layer with further relaxation to the exciton level. Detailed microscopic analysis of carrier capture in QDs<sup>11</sup> (taking into account semiconductor many-body physics) showed that the Coulomb scattering of electrons and holes, in delocalized states of the wetting layer, can provide efficient transitions into the discrete localized QD states. Also LO phonons can be an important mechanism responsible for such a relaxation. In this work, the pumping terms will represent only carrier capture due to phonons, processes where a fully correlated electron-hole pair is created in the QD.<sup>7</sup> Our aim, therefore, is not to make a systematic analysis of all the relaxation processes which are taking place in the system. Rather, it is to develop a heuristic model where one can investigate the impact of the different pumping mechanisms that we describe below and the relevance of QD inhomogeneities ( $\Delta_1 \neq \Delta_2$ ,  $g_1 \neq g_2$ ). In this framework, pumping is modeled by a coupling to a reservoir (that we denote by  $R$ ) of electrons, holes, and phonons. We consider two physically different situations for the pumping scheme, which we explain in what follows.

First, the case where the two QDs are distinguishable in a classical (as opposed to “quantum”) way for the pump exci-

tation. Such a situation arises when both QDs are far enough from each other to be resolved and pumped independently, or have very different excitation energies. This is the case when the *collection areas* around each dot—the areas of the wetting layer where free carriers are captured by the dot—are completely separated. In the following, we denote by  $A$  the collection areas of the dots (considered equal for simplicity) and  $A_c$  their overlapping area. Each of the QDs couple independently to each element of its own reservoir (electrons  $\hat{e}_{R_i}$ , holes  $\hat{h}_{R_i}$ , and phonons  $\hat{f}_{R_i}$ ), with coupling strengths  $\delta_{R_i}$ . This is the situation encountered with atoms and which has been more systematically explored.<sup>12</sup> The Hamiltonian of such a coupling reads

$$\hat{H}_{\text{pump}} = \sum_{R_1} [\delta_{R_1} \hat{\sigma}_1^+ \hat{e}_{R_1} \hat{h}_{R_1} \hat{f}_{R_1}^\dagger + \text{H.c.}] + \sum_{R_2} [\delta_{R_2} \hat{\sigma}_2^+ \hat{e}_{R_2} \hat{h}_{R_2} \hat{f}_{R_2}^\dagger + \text{H.c.}] \quad (3)$$

Applying the method and approximations of Refs. 7, 9, and 10, one arrives at two independent Lindblad terms of the form

$$\frac{P_{\text{ind}}}{2} \sum_{i=1,2} (2\hat{\sigma}_i^+ \hat{\rho} \hat{\sigma}_i^- - \hat{\sigma}_i^- \hat{\sigma}_i^+ \hat{\rho} - \hat{\rho} \hat{\sigma}_i^- \hat{\sigma}_i^+), \quad (4)$$

with parameters that we expect to be proportional to the collection areas  $A$  through the average injection efficiency per unit area and unit time  $\eta$ . This magnitude is proportional to the number of carriers in the wetting layer that actually create an exciton in the dot. Here, it is considered the same for both dots. The rate can then be expressed as  $P_{\text{ind}} = \eta A$ .

On the other hand, when, e.g., two identical dots are close to each other, if the coherence length of the excitation is larger than the distance between the two dots, the final state is a quantum superposition of the excited states of the QDs. This second situation of a common excitation bath has been considered, keeping the coherent nature of the couplings to the bath.<sup>14</sup> An analogous scheme of a common reservoir has been developed but for a common squeezed vacuum.<sup>15,16</sup> It requires the QDs to be indistinguishable for the pumping mechanisms (equal excitation energies  $\omega_1 = \omega_2$ ), the reservoir excitations—electron-hole pairs with high energy and phonons—to have a large enough coherence length to be shared by both dots, and the two collection areas to be fully overlapped ( $A = A_c$ ). With these characteristics, there is only one common reservoir and, given that we consider equal efficiencies for the dots (the excitation always affects both dots in the same way), only symmetrical states can be pumped. The Hamiltonian now reads

$$\hat{H}_{\text{pump}} = \sum_R [\delta_R (\hat{\sigma}_1^+ + \hat{\sigma}_2^+) \hat{e}_R \hat{h}_R \hat{f}_R^\dagger + \text{H.c.}] \quad (5)$$

Taking into account the fact that the reservoir is common,<sup>9,16</sup> we obtain two different contributions to the master equation:

(1) The first is an incoherent contribution to the dynamics given by a Lindblad term:

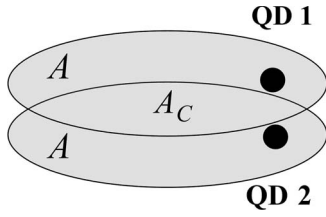


FIG. 2. Scheme of the two QDs with their associated collection areas  $A$ , which can be deformed by applying an electric field (Ref. 13). The overlapping area is called  $A_c$ . When it is nonzero and comparable to the coherence length of the excitation, cross-terms of the pump operators appear in the master equation.

$$\frac{P_{\text{com}}}{2} \sum_{i,j=1,2} (2\hat{\sigma}_i^+ \hat{\rho} \hat{\sigma}_j^- - \hat{\sigma}_j^- \hat{\sigma}_i^+ \hat{\rho} - \hat{\rho} \hat{\sigma}_j^- \hat{\sigma}_i^+), \quad (6)$$

with rate  $P_{\text{com}} = \eta A_c$ .

(2) The second is a direct coupling between the QDs, which appears as a coherent coupling in the Hamiltonian,  $H_{12} = g_{12}[\hat{\sigma}_1^+ \hat{\sigma}_2 + \text{H.c.}]$ , with  $g_{12}$  of the order of magnitude of the common pumping  $g_{12} \approx 2P_{\text{com}}$ . In the Dicke basis, this coupling detunes the state  $|T_0\rangle$  from  $|S\rangle$ .

In a more general and realistic case, the collection areas overlap partially in the region  $A_c$ , which contributes to the common pumping with a rate  $P_{\text{com}} = \eta A_c$ , while the rest of the areas  $A - A_c$  contribute to the excitation of each of the QDs separately with rates  $P_{\text{ind}} = \eta(A - A_c)$  (see Fig. 2). We define the degree of common pumping as the fraction  $C = A_c/A$ . Varying it between 0 and 1 interpolates between the two extreme cases of independent and common pumping. The Lindblad term of the total pumping is separated in two parts, one specific to each dot which depends on  $\hat{\sigma}_i^+$  and another one which is invariant under QD exchange (creates symmetrical states) and which can be expressed in terms of the operator  $\hat{J}^\pm = \hat{\sigma}_1^\pm + \hat{\sigma}_2^\pm$ . The total master equation of the system is now complete:

$$\begin{aligned} \frac{d\hat{\rho}}{dt} = & i[\hat{\rho}, \hat{H}_0] + i[\hat{\rho}, \hat{H}_{12}] + \left[ \frac{\kappa}{2} \mathcal{L}_{\hat{a}} + \frac{\gamma}{2} (\mathcal{L}_{\hat{\sigma}_1^-} + \mathcal{L}_{\hat{\sigma}_2^-}) \right] \hat{\rho} \\ & + \left[ \frac{P_{\text{ind}}}{2} \mathcal{L}_{\hat{\sigma}_1^+} + \frac{P_{\text{ind}}}{2} \mathcal{L}_{\hat{\sigma}_2^+} + \frac{P_{\text{com}}}{2} \mathcal{L}_{\hat{J}^+} \right] \hat{\rho}. \end{aligned} \quad (7)$$

As a summary, the first line describes the coherent dynamics of the two dots and the cavity, including the direct QD coupling created by the common excitation bath ( $\hat{H}_{12}$ ). The second line describes in the usual way the losses of cavity photons and QD excitations. The third line describes the incoherent pumping written here to set apart clearly the two schemes which play an important role in our analysis: first, the pumping of each dot regardless of the other, at rate  $P_{\text{ind}}$ , and then the joint pumping, which distributes the excitation among the two dots as a symmetrical quantum superposition, at rate  $P_{\text{com}}$ . As proved in the next section, one would expect this common pumping mechanism to create new correlations and coherent superposition between the dots. Taking advantage of this situation, we will show how to build up entanglement between the QD excited states. On the other hand, we

find the incoherent independent pumping—that cannot increase coherence between dots—more suitable for lasing properties.

In this work, we are interested in the properties of the steady state of Eq. (7) in the limit of strong coupling between cavity and QDs. The strong coupling regime occurs when the interaction between matter and light overcomes the radiative losses of the cavity and new dressed eigenstates appear in the system, namely, the oscillations between QD and cavity excitations (see Ref. 2 for a review). In this regime, decay rates  $\kappa$  and  $\gamma$  are small, while the coupling  $g$  between dots and cavity is high enough so that  $\kappa, \gamma \ll g$ . The parameter  $g$  depends on both the properties of the cavity and the emitters:  $g \sim (f/V)^{-1/2}$ , where  $V$  is the effective cavity volume and  $f$  the oscillator strength of the emitter. Therefore, in order to achieve strong coupling experimentally, the cavity must have a high quality factor  $Q$  ( $\kappa \sim Q^{-1}$ ) and a small effective volume  $V$ . The emitters must be placed close to the antinode of the electric field in the cavity, have transition frequencies close to resonance with the cavity mode, and exhibit high oscillator strengths.

In the strong coupling regime, there exists a steady state for the system when the losses are compensated by the pump and some population is sustained in time. This state was obtained in two independent and equivalent ways. First, we solved the set of linear equations for the density matrix elements resulting from setting the time derivative to zero  $d\hat{\rho}/dt = 0$ .<sup>17</sup> Second, we time-integrated the master equation and waited a time long enough to reach the steady state. The solution is unique for a given set of parameters, regardless of the initial state, and both methods agreed exactly except when a singularity arises (as detailed in the next section), which can only be reached asymptotically with the time-integrated approach.

### III. ENTANGLEMENT: TANGLE AND ENTROPY

Two degrees of freedom are entangled when the system density matrix cannot be expressed as a mixture of separable states.<sup>18</sup> Besides their fundamental interest, entangled states are highly sought for applications in quantum information processing. Many such implementations might involve QDs as building blocks.<sup>19,20</sup> In the following, we consider the possibilities open to the system under consideration.

From the couplings that Eq. (7) establishes between the different levels in the local basis, it follows that the reduced density matrix for the QDs in the steady state takes the form

$$\hat{\rho}_{\text{QD}}(t \rightarrow \infty) = \begin{pmatrix} \rho_{00} & 0 & 0 & 0 \\ 0 & \rho_{11} & \rho_{12} & 0 \\ 0 & \rho_{12}^* & \rho_{22} & 0 \\ 0 & 0 & 0 & \rho_{33} \end{pmatrix}. \quad (8)$$

Therefore, the only way to entangle the two dots is to populate the Dicke states  $|T_0/S\rangle = (|1\rangle \pm |2\rangle) / \sqrt{2}$  (which are two of the so-called Bell states). In a bipartite four-level system, the degree of entanglement can be quantified by the *tangle* ( $\tau$ ),<sup>21</sup> which ranges from 0 (separable states) to 1 (maximally entangled states). In order to compute  $\tau$ , we need to introduce

the intermediate quantities  $\hat{T}$  and  $\hat{R}$ , defined as

$$\hat{T} = \begin{pmatrix} 0 & 0 & 0 & -1 \\ 0 & 0 & 1 & 0 \\ 0 & 1 & 0 & 0 \\ -1 & 0 & 0 & 0 \end{pmatrix} \quad \text{and} \quad \hat{R} = \hat{\rho}_{\text{QD}} \hat{T} \hat{\rho}_{\text{QD}}^* \hat{T}. \quad (9)$$

The tangle is then

$$\tau = [\max\{0, \sqrt{\lambda_1} - \sqrt{\lambda_2} - \sqrt{\lambda_3} - \sqrt{\lambda_4}\}]^2, \quad (10)$$

where  $\{\lambda_1, \lambda_2, \lambda_3, \lambda_4\}$  are the eigenvalues in decreasing order of  $\hat{R}$ . One finds that whenever it is not zero, the tangle is given by

$$\tau = 4(|\rho_{12}| - \sqrt{\rho_{00}\rho_{33}})^2. \quad (11)$$

We are interested in conditions that maximize  $\tau$ : these correspond to large values of the off-diagonal elements  $|\rho_{12}|$  and small populations of the states  $|0\rangle, |3\rangle$ . Here, dissipation and pumping cause  $\hat{\rho}_{\text{QD}}$  to evolve into a mixture, with reduced coherences and nonzero occupancy of all levels. This limits the maximum tangle that can be achieved.<sup>22</sup> In order to isolate the contribution of such effect, we quantify the degree of purity of the QD states by computing the *linear entropy*:

$$S_L = \frac{4}{3}[1 - \text{Tr}(\hat{\rho}_{\text{QD}}^2)] = \frac{4}{3}[1 - (\rho_{00}^2 + \rho_{11}^2 + \rho_{22}^2 + \rho_{33}^2 + 2|\rho_{12}|^2)], \quad (12)$$

which is 0 for a pure state and 1 for a maximally disordered state (where the four dot states have the same probability 1/4).

The entangling of the dots in the singlet state (rather than the triplet) is a natural way to achieve a good degree of tangle and purity at the same time, as in the limiting case where parameters for each dot are identical ( $g_1 = g_2$ ,  $\Delta_1 = \Delta_2$ ) the singlet becomes a dark state. In the case where  $P_{\text{ind}} = 0$ , it is also decoherence free,<sup>23</sup> i.e., is not affected by the decoherence introduced by the pump.<sup>24</sup> When the limiting case is only approached ( $g_1 \approx g_2$ ),  $|S\rangle$  becomes coupled to the triplet subspace by a small effective coefficient  $\delta g$  (see Fig. 1, and the dots can be trapped in the singlet state (see below). As we already mentioned, equivalent trapping mechanisms have been reported when interacting with a common squeezed bath.<sup>15,16</sup> Therefore, our proposal for achieving a high value of the tangle is based on a slight imbalance between the coupling strengths of the QDs, resulting in a very high occupation of the singlet state.

In Fig. 3, we plot the mean number of photons and the population of the singlet state (inset) for  $\Delta_i = 0$ . The first dot is in the strong coupling regime with the cavity ( $\kappa/g_1 < 4$ ), whereas the second one goes from a weak to a strong coupling regime as a function of  $g_2$ . If the QDs are pumped independently (red line), the photon number increases with  $g_2$  until the maximum is reached for  $g_2 = g_1$ . The presence of the second dot in strong interaction with the cavity increases nonlinearly the emission (see below).

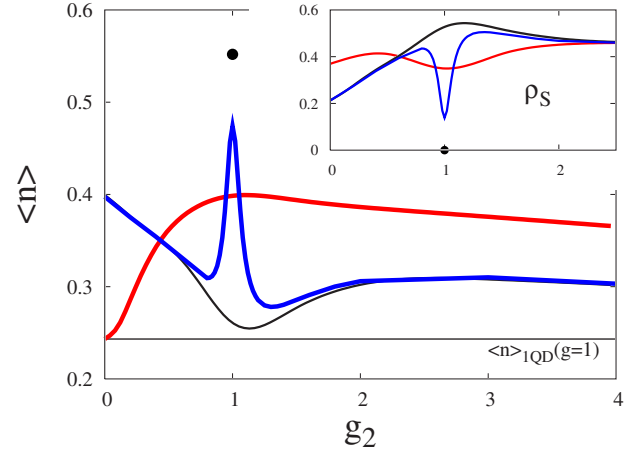


FIG. 3. (Color online) Mean number of photons  $\langle n \rangle$  stored in the cavity as a function of the coupling of the second dot  $g_2$  for  $\kappa = 1$ ,  $\Delta_1 = \Delta_2 = 0$ , and  $P = 0.33$  (all in units  $g_1$ ). Both the cases of independent pumping only (red line, corresponding to  $P_{\text{ind}} = P$  and  $P_{\text{com}} = 0$ ) and common pumping only (black and blue lines, with  $P_{\text{ind}} = 0$  and  $P_{\text{com}} = P$ ) are plotted. In the latter case, the black line corresponds to  $\gamma = 0$  and the blue one to  $\gamma = 5 \times 10^{-3}$ . The reference value of one QD in the cavity with  $g = 1$  is given. Inset: Population of the singlet state. In both plots, the black line has a discontinuity at  $g_1 = g_2$ . The singular value assumed by  $\langle n \rangle$  and the singlet population in this case is marked by the black point.

On the other hand, when the pump is common, a very different behavior is observed (blue line in Fig. 3). First, for  $g_2 = 0$ , the single-QD limit is not recovered, since the cross pumping term  $P_{\text{com}}$  creates an effective coupling between the QDs, which induces correlation between their states even when no cavity-induced coupling is present. The other striking difference occurs for  $|g_2 - g_1| \approx 0$ : the photon number decreases, while the singlet population increases. Here,  $\delta g \ll g$ , and the singlet is almost decoupled from the dynamics (see Fig. 1 and the above discussion). There is a slow flow of population into the singlet state with zero photons, which also has a very long relaxation time. In the specific case  $g_2 = g_1$ , there is an abrupt change of the photon number, and the system turns into an effective three-level system, as the singlet is optically dark.

The strong differences between the emission of a system under independent or common pumping evidenced in Fig. 3 especially when one of the dots is not coupled to the cavity or when they are coupled in a similar way) provide a simple experimental hint to discriminate them.

In the case where the only decay channel for the dot is the emission into the cavity mode ( $\gamma = 0$ ), this behavior is singular (black in Fig. 3). For finite  $\gamma$ , the singularity is replaced by an abrupt maximum. The occupation of state  $|T_0\rangle$  is enhanced. However, this state being strongly coupled with the other two triplet states, the purity is not high and the tangle remains zero. Therefore, in order to increase  $\tau$ , we seek the set of parameters that maximize the singlet occupation, knowing that a moderate population of triplet states does not suffice (Fig. 3). The best regime corresponds to small  $\delta g/g$  and large ratios  $g/\kappa$ . Besides, in order to keep at a minimum the excitations of radiant states in such a configuration, the

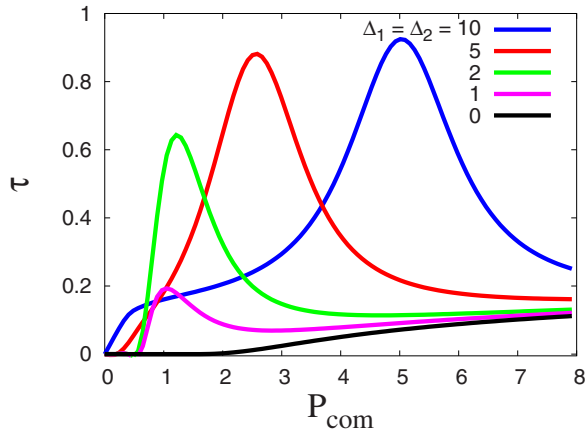


FIG. 4. (Color online) Tangle  $\tau$  for various detunings as a function of  $P_{\text{com}}$ . Parameters:  $\kappa=1$ ,  $\gamma=5 \times 10^{-3}$ ,  $P_{\text{ind}}=0$ , and  $g_2=0.6$  (all in units of  $g_1$ ). The maximum tangle achieved grows with the detuning, but requires a larger pumping.

QDs must be detuned from the cavity mode. In turn, because of this detuning, which weakens the dynamics, the pumping must be increased. Accordingly, we show the tangle  $\tau$  for  $g_2=0.6$ ,  $\kappa=1$ , and  $\gamma=5 \times 10^{-3}$  (all in units of  $g_1$ ) as a function of the pumping  $P_{\text{com}}$  (Fig. 4). Larger detunings increase the tangle, though this requires larger values of the pump as well. For very high values of the pump, the emission from the two dots gets quenched<sup>24</sup> and the number of cavity photons vanishes. The population saturates between the states  $|S,0\rangle$  and  $|T_1,0\rangle$  (with zero photon) and the tangle gets

spoiled. There is, therefore, a maximum for a given detuning, as shown in Fig. 4 from the numerical results.

In the following, we consider a detuning  $\Delta=2$  between the dots and the cavity mode, so as to keep realistic values of the pump required to maximize the tangle, namely,  $P_{\text{com}}=1.22$  as read from the magenta line in Fig. 4. In Fig. 5, we make a systematic analysis of the steady state in terms of (a) its cavity population, (b) population of the singlet state with zero photon  $|S,0\rangle$  (almost equal to the total population of the singlet), (c) tangle, and (d) entropy, by scanning the space of relevant parameters  $g_2$  and  $P_{\text{com}}$ , and keeping other parameters fixed to the values given above. The maximum of the tangle ( $\tau=0.64$ , marked with a cross) is achieved at  $g_2=0.6$  and  $P_{\text{com}}=1.22$  (see Fig. 4). It corresponds to the minimum entropy and an increase of the population of the state  $|S,0\rangle$ , and therefore, to a decrease of  $\langle n \rangle$ .

Entanglement between the QD excited states is not an easy magnitude to access experimentally (other than by reconstructing the QD density matrix with quantum tomography). The low number of cavity photons associated with the maximum of the tangle, and consequently, the low cavity emission, can be used as an experimental indication of a high degree of entanglement.

Another important feature of these plots (Fig. 5) is that they are not symmetric with respect to  $g_2=g_1$ , and in this case, it is easier to reach the maximum tangle when the second dot coupling is smaller than the first. The sign of  $g_1-g_2$ , which maximizes the tangle for a given  $|g_1-g_2|$ , depends on the position of the maxima in the curves of  $\langle n \rangle$  and singlet population with respect to  $g_2$  around the singularity

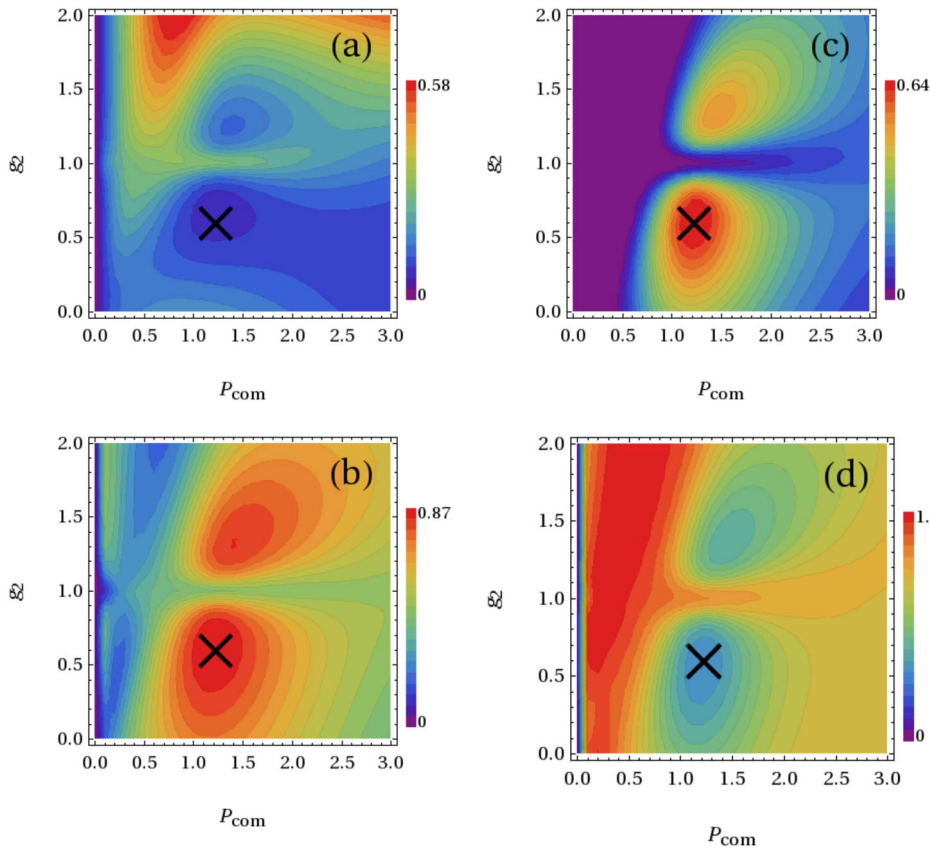


FIG. 5. (Color online) Density plots of (a) mean number of photons, (b) population of the state  $|S,0\rangle$ , (c) tangle, and (d) entropy, all as a function of  $g_2$  and  $P_{\text{com}}$ . Parameters are  $\kappa=1$ ,  $\gamma=5 \times 10^{-3}$ ,  $\Delta_1=\Delta_2=2$ , and  $P_{\text{ind}}=0$  (all in units of  $g_1$ ). The maximum value for the tangle ( $\tau=0.64$ ) is achieved at  $g_2=0.6$  and  $P_{\text{com}}=1.22$  (this point is marked with a cross).

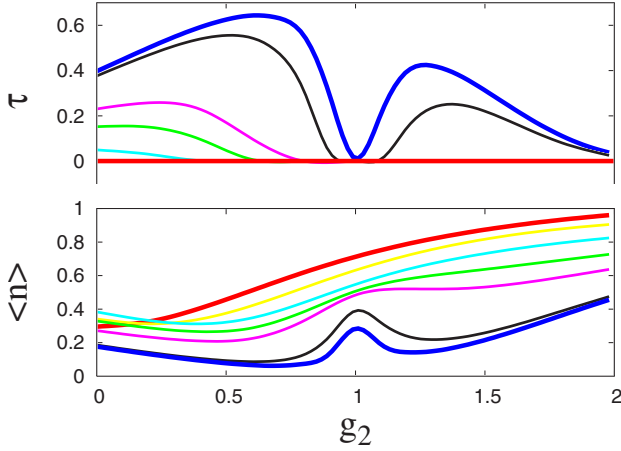


FIG. 6. (Color online) Tangle and mean number of photons as a function of  $g_2$  for  $\kappa=1$ ,  $\Delta_1=\Delta_2=2$ ,  $\gamma=5 \times 10^{-3}$ , and total pump of 1.22 (all in units of  $g_1$ ). The cases from independent pump  $C=0$  (red) to common pump  $C=1$  (dark blue) are considered. The intermediate curves correspond to  $C=0.33$  (yellow),  $0.66$  (light blue),  $0.82$  (green),  $0.91$  (magenta), and  $0.99$  (black).

$g_1=g_2$ . The best case is the one which maximizes the singlet population and minimizes the total population.

In Fig. 6—the counterpart of Fig. 3 in the configuration under consideration, which is suitable for entanglement—these maxima are obtained for  $g_2 < g_1$ . Note that in Fig. 3 the situation is opposite. Note also that a very strong coupling of the QDs with the cavity is not needed. Figure 6 shows as well the transition from the common bath ( $C=1$ ) to independent ones ( $C=0$ ); in the case where the total pump is fixed,  $P_{\text{ind}}+P_{\text{com}}=1.22$ . It gives an idea of the overlap needed to obtain a sizable tangle. No tangle is obtained for an overlap less than 66%. The important overlap which is required can be obtained experimentally by the application of an electric field which can squeeze the areas of two nearby QDs into each other.<sup>13</sup>

#### IV. LASING: MEAN NUMBER OF PHOTONS AND SECOND-ORDER COHERENCE

In this section, we analyze the lasing properties of the above system. A practical motivation is the significant improvement, as far as low threshold behavior is concerned, recently obtained by a system having just a few (from 2 to 4) QDs embedded in a single-mode microcavity<sup>25</sup> with respect to previous attempts using quantum wells or high density QDs.<sup>26–31</sup> An important finding in this section is that the presence of a second dot, even far from resonance with the cavity, changes substantially the emission of a single one.

As opposed to the previous section, we now focus on the quantum state of the cavity photons, rather than on that of the QDs. Nevertheless, the light state depends on the coherences established between the levels of the system, and therefore, depends on the QD parameters. Unlike atoms, QDs can be differently detuned with respect to the cavity mode. In what follows, we therefore study the dependence on the detuning configuration of the mean photon number

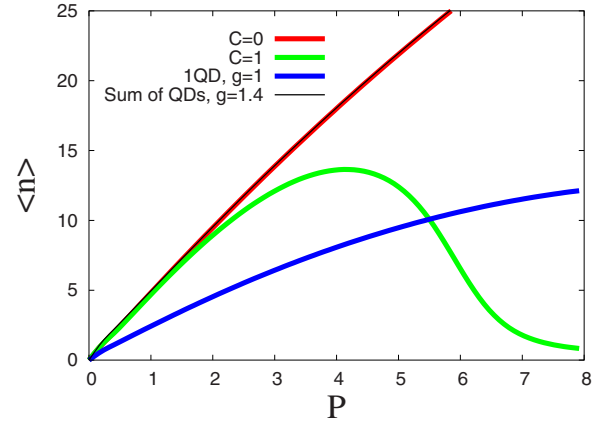


FIG. 7. (Color online) Mean number of photons stored in the cavity as a function of pumping  $P$  for  $\kappa=0.2$ ,  $\gamma=5 \times 10^{-3}$ , and  $g_1=g_2=1$ . Both cases, with independent ( $P_{\text{ind}}=P$  and  $P_{\text{com}}=0$ , red) and common pumping ( $P_{\text{ind}}=0$  and  $P_{\text{com}}=P$ , green), are presented for the resonant case ( $\Delta_1=\Delta_2=0$ ). These are compared with the emission of a single QD in resonance with coupling  $g=1$  (blue line), and the sum of emissions of two independent dots in resonance with renormalized coupling constants  $g=\sqrt{2}$  (black line).

and of the second-order coherence function in the case of zero delay  $g^{(2)}(0)=1+(\Delta n^2-\langle n \rangle)/\langle n \rangle^2$  ( $\Delta n$  is the standard deviation of the photon distribution). Only in the case where the two dots are equally detuned, one can compare the two limiting pumping schemes described previously; as mentioned above, such symmetry is a necessary condition for the common pumping bath.

Given the structure of Eq. (7), all off-diagonal elements of the density matrix between levels with equal QD states but different number of photons have been washed away in the steady state. Therefore, the photon reduced density matrix  $\hat{\rho}_{\text{ph}}=\text{Tr}_{\text{QD}}\{\hat{\rho}\}$  is diagonal in the number of photons: it is, thus, impossible for the system to achieve a coherent state,

$$\hat{\rho}_\alpha = |\alpha\rangle\langle\alpha| = e^{-|\alpha|^2} \sum_{n,m} \frac{\alpha^n \alpha^{*m}}{\sqrt{n!m!}} |n\rangle\langle m|, \quad (13)$$

at the steady state. However, the system can reach a mixture of number states with the same Poissonian distribution

$$\hat{\rho}_P = e^{-|\alpha|^2} \sum_n \frac{|\alpha|^{2n}}{n!} |n\rangle\langle n| \quad (14)$$

as happens for a laser much above threshold.<sup>32</sup> In both cases,  $\langle n \rangle = |\alpha|^2$  and  $g^{(2)}(0)=1$ .

Fixing the leaky modes to  $\gamma=5 \times 10^{-3}$  and the coupling constants  $g_2=g_1=1$ , we first compare the number of photons  $\langle n \rangle$  in the cases where one or two QDs are in resonance with the cavity (Fig. 7). Figure 7 shows how the growth of the occupation number with pumping is limited by the *self-quenching effect*.<sup>7,24</sup> This results in a maximum cavity population, corresponding to an optimum value of the pumping intensity. Further increase of the pumping results in a decrease of the mean number of photons and saturation of the dots. This effect is due to the incoherent nature of the pump,

which destroys the coherences established between QDs and cavity. The off-diagonal elements between states belonging to each manifold with the same number of excitations are killed, driving the system to a thermal state [ $g^{(2)}(0)=2$ ]. However, we are interested in the behavior at much lower pumps, where the number of photons does not yet saturate, as is the case experimentally.<sup>25</sup>

In the pumping range plotted in Fig. 7, the self-quenching region is reached only for the case of a common pumping bath (green line). Therefore, this case is the least suitable for lasing properties. There are several reasons for the enhancement of the self-quenching effect in this case. The first reason is that by neglecting the leaky modes, the QD system is reduced from four to three levels, diminishing the range of pump available before reaching the saturation of the ensemble. Taking into account leaky modes, the second reason is that, although  $g_1=g_2$ , and thus the singlet is not coherently coupled to the triplet, the decay of state  $|T_1, 0\rangle$  into  $|S, 0\rangle$  via those leaky modes populates the singlet, thus hindering the storage of photons. A third drawback is the presence of the coherent coupling between states  $|1\rangle$  and  $|2\rangle$ , which prevents the distribution of photons from being Poissonian. The resulting distribution is a sum of the contribution of the singlet subspace (with high probabilities around zero photons) and the triplet (Poissonian-like distributions as found in the other cases plotted here).

On the other hand, in the case of independent pumpings, the emission of two QDs approximately corresponds to the sum of the individual emissions with coupling constants renormalized by a factor  $\sqrt{2}$ . This approximation improves when both dots are close to resonance, as shown by the red curve in Fig. 7. The second-order coherence function is also similar at low pumping.

As the common bath of excitations is detrimental to lasing, we now consider the case of independently and equally pumped dots only ( $P_{\text{com}}=0$  and  $P_{\text{ind}}=P$ ), where QDs are coupled uniquely through the cavity mode. Results are given in Fig. 8, which shows the behavior of  $\langle n \rangle$  and  $g^{(2)}(0)$  as a function of the pump for different detuning configurations: equal ( $\Delta_1=\Delta_2$ ), opposite ( $\Delta_1=-\Delta_2$ ), and mixed ( $\Delta_1=0 \neq \Delta_2$ ) detunings.

In the ideal case, if the QDs are in resonance (Fig. 7), the production of photons is very efficient, and the second-order coherence function is always 1 until the self-quenching begins. With detuning, a threshold for linear production of photons (as a function of pumping) appears, as can be seen in the figure. It occurs approximately when the pumping compensates the losses: the number of photons becomes larger than 1 and the stimulated emission exceeds the spontaneous one. This transition into lasing is accompanied by the decrease of the second-order coherence function to a value of 1 [Fig. 8(b)] and a Poissonian distribution of the photon number [a matrix of the form Eq. (14)]. The effect is also present in the case with one dot, but the threshold of the transition is considerably lowered by the presence of a second dot.

The optimal configurations, i.e., the ones with lowest threshold, are those where at least one of the dots is in resonance. In these case, the presence of the second dot makes a great difference even if its detuning is large. So, neglecting

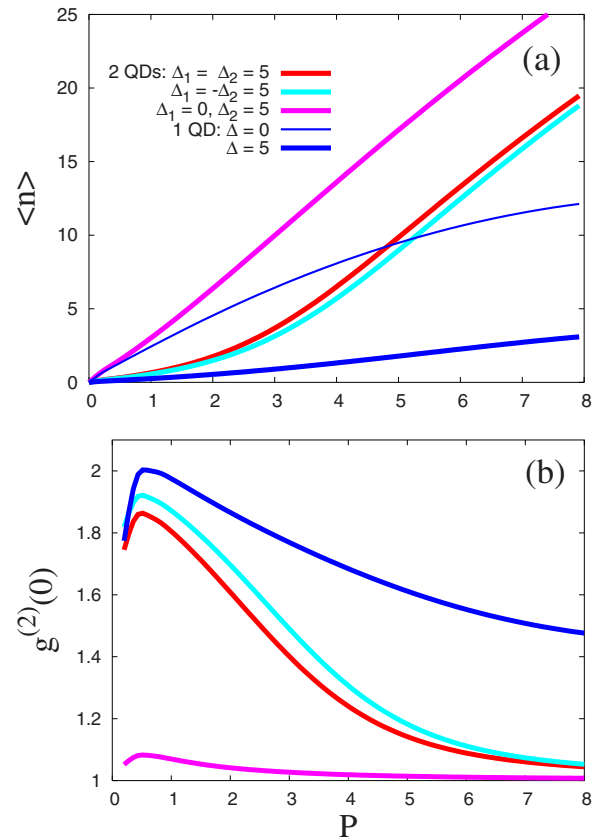


FIG. 8. (Color online) (a) Mean number of photons  $\langle n \rangle$  stored in the cavity and (b) second-order coherence function  $g^{(2)}(0)$  of the cavity field, as a function of  $P_{\text{ind}}=P$ , for  $P_{\text{com}}=0$ ,  $\kappa=0.2$ ,  $\gamma=5 \times 10^{-3}$ , and  $g_2=1$ . Several detuning cases are presented, with equal ( $\Delta_1=\Delta_2=5$ ), opposite ( $\Delta_1=-\Delta_2=5$ ), and mixed ( $\Delta_1=0, \Delta_2=5$ ) configurations. There is a qualitative change with two dots as, even when none is in resonance with the cavity mode, the threshold for lasing (with linear increase of  $\langle n \rangle$  with  $P$ ) is low also in the case where the single dot alone would not lase.

the role of QDs out of resonance (as done in a more sophisticated framework<sup>33</sup>) is not a good approximation. We can see this by comparing  $\langle n \rangle$  of one QD in resonance [thin blue line in Fig. 8(a)] with two dots, one in resonance and the second highly detuned [ $\Delta_1=0$  and  $\Delta_2=5$ , magenta line in Fig. 8(a)]. Whether the detunings are identical ( $\Delta_1=\Delta_2$ ) or opposite ( $\Delta_1=-\Delta_2$ ) makes no qualitative difference, although the two cases are not strictly equal.

In these results, we find an explanation for the recent experimental findings<sup>25</sup> on lasing, with unexpected low laser thresholds and high photon production efficiency from a cavity containing a few dots out from resonance. The experimental parameters in that case are comparable to ours (with a pump threshold of  $P=0.08$  meV), as well as the detunings of the dots,  $\Delta_1 \approx -\Delta_2 \approx 5$  meV. In our scheme, several dots result in qualitative changes of the emission, enhancing it significantly even when dots are off-resonance. In this sense, our model predicts still better cavity emission with extremely low threshold if one dot could be matched in resonance with the cavity.

## V. CONCLUSIONS

We have investigated the steady state properties of two QDs in a microcavity, for which we developed a model where the QDs are pumped either in an independent or in a common fashion. We have shown that the general case is a mixture of the two kinds of pumping, which is determined mainly by geometrical factors, but can be increased one way or the other, for instance, by applying an external electric field.

In the case where the dots are essentially excited through the common pumping, quantum interferences in the dots alter significantly the dynamics and yield singularities or abrupt features in the steady state populations. For suitable sets of parameters, which include different couplings between cavity and dots, the system can be brought to a regime where the singlet state,  $|S\rangle = (|E_1, G_2\rangle - |G_1, E_2\rangle) / \sqrt{2}$ , is predominantly occupied. This provides good values of the tangle despite the incoherent and continuous nature of the pumping.

In the case where the dots are essentially pumped independently, the presence of a largely detuned or weakly

coupled dot changes qualitatively the dynamics of a near resonant, strongly coupled dot. In view of its lasing properties, the system therefore acquires a low stimulated emission threshold, resulting in efficient cavity population with Poissonian distribution, even when both dots are detuned from the cavity mode. This is qualitatively different from a model with isolated dots, the emission of which would scale with their number, especially at nonzero detuning.

Finally, we would like to stress that our results can be applied to situations in which qubits are physically built up by means of other systems as, e.g., atoms flowing through a cavity or superconducting qubits in microwave resonators.

## ACKNOWLEDGMENTS

This work has been partly supported by the Spanish MEC under Contracts Nos. Consolider-Ingenio2010 CSD2006-0019, MAT2005-01388, and NAN2004-09109-C04-4, by CAM under Contract No. S-0505/ESP-0200, and by the Italy-Spain “integrated action” HI2005-0027. F. Troiani acknowledges financial support from MIUR under FIRB Contract No. RBIN01EY74.

- 
- <sup>1</sup>A. İmamoğlu, Opt. Photonics News **13**, 22 (2002).  
<sup>2</sup>G. Khitrova, H. M. Gibbs, M. Kira, S. W. Koch, and A. Scherer, Nat. Phys. **2**, 81 (2006).  
<sup>3</sup>K. Hennessy, A. Badolato, M. Winger, D. Gerace, M. Atature, S. Gulde, S. Fält, E. L. Hu, and A. İmamoğlu, Nature (London) **445**, 896 (2007).  
<sup>4</sup>A. Badolato, K. Hennessy, M. Atature, J. Dreyser, E. Hu, P. M. Petroff, and A. İmamoğlu, Science **308**, 1158 (2005).  
<sup>5</sup>A. Rastelli, A. Ulhaq, S. Kiravittaya, L. Wang, A. Zrenner, and O. G. Schmidt, Appl. Phys. Lett. **90**, 073120 (2007).  
<sup>6</sup>O. Gywat, F. Meier, D. Loss, and D. D. Awschalom, Phys. Rev. B **73**, 125336 (2006).  
<sup>7</sup>J. I. Perea, D. Porrás, and C. Tejedor, Phys. Rev. B **70**, 115304 (2004).  
<sup>8</sup>E. Jaynes and F. Cummings, Proc. IEEE **51**, 89 (1963).  
<sup>9</sup>D. F. Walls and G. J. Milburn, *Quantum Optics* (Springer-Verlag, Berlin, 1994).  
<sup>10</sup>F. Troiani, J. I. Perea, and C. Tejedor, Phys. Rev. B **74**, 235310 (2006).  
<sup>11</sup>T. R. Nielsen, P. Gartner, and F. Jahnke, Phys. Rev. B **69**, 235314 (2004).  
<sup>12</sup>G. Yeoman and G. M. Meyer, Phys. Rev. A **58**, 2518 (1998).  
<sup>13</sup>P. O. Holtz, Proceedings of the PLMCN7 Conference, Havana, 2007 (unpublished).  
<sup>14</sup>D. Braun, Phys. Rev. Lett. **89**, 277901 (2002).  
<sup>15</sup>Z. Ficek and R. Tanas, Phys. Rep. **372**, 369 (2002).  
<sup>16</sup>U. Akram, Z. Ficek, and S. Swain, Phys. Rev. A **62**, 013413 (2000).  
<sup>17</sup>E. del Valle, F. P. Laussy, F. Troiani, and C. Tejedor, Superlattices Microstruct. (to be published).  
<sup>18</sup>M. A. Nielsen and I. L. Chuang, *Quantum Computation and Quantum Information* (Cambridge University Press, Cambridge, England, 2000).  
<sup>19</sup>D. D. Awschalom, D. Loss, and N. Samarth, in *Semiconductor Spintronics and Quantum Computation* (Springer-Verlag, New York, 2002).  
<sup>20</sup>A. İmamoğlu, D. D. Awschalom, G. Burkard, D. P. DiVincenzo, D. Loss, M. Sherwin, and A. Small, Phys. Rev. Lett. **83**, 4204 (1999).  
<sup>21</sup>W. K. Wootters, Phys. Rev. Lett. **80**, 2245 (1998).  
<sup>22</sup>W. J. Munro, D. F. V. James, A. G. White, and P. G. Kwiat, Phys. Rev. A **64**, 030302(R) (2001).  
<sup>23</sup>D. A. Lidar, I. L. Chuang, and K. B. Whaley, Phys. Rev. Lett. **81**, 2594 (1998).  
<sup>24</sup>O. Benson and Y. Yamamoto, Phys. Rev. A **59**, 4756 (1999).  
<sup>25</sup>S. Strauf, K. Hennessy, M. T. Rakher, Y. S. Choi, A. Badolato, L. C. Andreani, E. L. Hu, P. M. Petroff, and D. Bouwmeester, Phys. Rev. Lett. **96**, 127404 (2006).  
<sup>26</sup>R. E. Slusher, A. F. J. Levi, U. Mohideen, S. L. McCall, S. J. Pearton, and R. A. Logan, Appl. Phys. Lett. **63**, 1310 (1993).  
<sup>27</sup>L. H. Zhang and E. Hu, Appl. Phys. Lett. **82**, 319 (2003).  
<sup>28</sup>H.-G. Park, S.-H. Kim, S.-H. Kwon, Y.-G. Ju, J.-K. Yang, J.-H. Baek, S.-B. Kim, and Y.-H. Lee, Science **305**, 1444 (2004).  
<sup>29</sup>O. Painter, R. K. Lee, A. Scherer, A. Yariv, J. D. O’Brien, P. D. Dapkus, and I. Kim, Science **284**, 1819 (1999).  
<sup>30</sup>M. Rohener, J. P. Reitmaier, A. Forchel, F. Schaefer, and H. Zull, Appl. Phys. Lett. **71**, 488 (1997).  
<sup>31</sup>H. Y. Ryu, M. Notomi, E. Kuramoti, and T. Segawa, Appl. Phys. Lett. **77**, 184 (2000).  
<sup>32</sup>L. Mandel and E. Wolf, *Optical Coherence and Quantum Optics* (Cambridge University Press, New York, 1995).  
<sup>33</sup>C. Gies, J. Wiersig, M. Lorke, and F. Jahnke, Phys. Rev. A **75**, 013803 (2007).